Forest Chemicals Review
www.forestchemicalsreview.com
ISSN: 1520-0191
May-June 2022 Page No. 1348 – 1367
Article History: Received: 24 February 2022, Revised: 05 April 2022, Accepted: 08 May 2022, Publication: 30 June 2022

Analysis of Steering Performance of Arch Waist Agricultural Travelling Chassis with Dual Power Flow Differential Steering Mechanism

Lingxin Geng, Jiajie Guo*, Xiaolin Xie*, Xiaobing Han, Yuchao Li, Zixiang Yan, Yibo Qin
College of Agricultural Equipment Engineering, Henan University of Science and Technology, Luoyang, Henan, China
*Corresponding Author.

Abstract:

The steering mechanism directly affects the steering performance and operational efficiency of agricultural machinery. The conventional differential steering mechanism applies to a limited number of turning radii and often requires components such as brakes. Therefore, a dual power flow differential steering mechanism has been designed to enable arch waist agricultural travelling chassis to achieve in-situ steering and any turning radius on any terrain. We established the kinematic model for the differential steering mechanism's output shaft rotational velocity (input) of the gearbox, shaft rotational velocity of the steering motor (input), and the rotational velocity of the two semi shafts (output). The kinematic model for the output shaft rotational velocity (input) of the gearbox, shaft rotational velocity (input) of the steering motor and turning radius was obtained based on the relationship between the rotational velocities of two semi shafts and the turning radius of the arch waist agricultural travelling chassis. Additionally, we set up the dynamics model for the differential steering mechanism's output shaft torque (input) of the gearbox, shaft torque of the steering motor (input) and the torque of the two semi-shafts (output). Finally, the differential steering mechanism was installed on the arch waist agricultural travelling chassis to test the steering performance on the concrete pavement and farmland. The test results revealed that the prototype has good straight-line stability, with a yaw rate of 0.82%, which is in line with the national standard. The average minimum radius for in-situ steering on the concrete pavement is 0.033 m. The average minimum radius for operation on the farmland is 0.040 m, effectively reducing the contact area between the ground and the prototype. Therefore, it can be widely used in complex terrains such as hills and mountains.

Keywords*: Agricultural machinery, Dual power flow, Differential steering mechanism,Dynamics model, Kinematic model.*

I. INTRODUCTION

Hilly and mountainous areas account for more than 43% of China's territory. The agricultural mechanization in these areas has long fallen behind than that in plain areas due to the complex environment, large height differences between adjacent plots, irregular shape, and narrow roads. To fully realize agricultural mechanization and intellectualization, China is in sore need of enhancing the operational performance and efficiency of agricultural machinery in hilly and mountainous areas [1, 2].

Forest Chemicals Review
www.forestchemicalsreview.com
ISSN: 1520-0191
May-June 2022 Page No. 1348 – 1367
Article History: Received: 24 February 2022, Revised: 05 April 2022, Accepted: 08 May 2022, Publication: 30 June 2022

In hilly and mountainous areas, the steering performance of agricultural machinery is more important than its straight-line stability. The flexible steering performance and the good straight-line stability directly affect the operational efficiency of agricultural machinery in the hilly and mountainous areas [3]. The steering maneuver, terrain feature, driving speed, travelling chassis localization, steering mechanism, etc., influence the steering performance during driving, which significantly affects the steering performance of agricultural machinery [4-10]. A host of scholars have conducted numerous studies on the steering of tracked vehicles. Wong analyzed the steering principle of tracked vehicles without considering the track slip caused by the speed difference between the two sides of the tracks during the steering process [11, 12]. G.M. et al. [13] built a kinematic model of tracked vehicles based on the instantaneous center of rotation when exploring the motion of the part of the tracked vehicle in contact with the ground. Dong Chao et al. [14] took into account centrifugal force and track slip (skid) and developed a mathematical model for the steering of tracked vehicles. The steering mechanism of tracked machinery is classified into a single power flow steering mechanism and dual power flow steering mechanism [15] according to the difference of power transmission. The most widely used single power flow steering mechanisms are the steering clutch mechanism, planetary mechanism, single differential mechanism and dual differential mechanism. The single power flow steering mechanism has obvious shortcomings. For example, the vehicle has only a few fixed turning radii. If the steering is not performed according to the prescribed radius, it needs to rely on the sliding between the friction elements. In this process, a large amount of heat and wear is generated, making it difficult to obtain a stable turning radius and good reliability. Besides, it causes a large power loss [16]. Dual power flow separates linear and steering power, with a certain degree of independence. The main feature is that there is no speed difference between the two sides during linear driving. However, when steering, the vehicle changes its direction through the steering mechanisms, mainly the mechanical dual power flow differential steering mechanism and hydraulic mechanical differential steering mechanism, to form the speed difference between the two sides of the track superposed by linear driving speeds of different gears. Although the hydro-mechanical dual power flow differential steering system has an infinite number of steering radii compared to the single power flow steering system, substantially improving the driving mobility and flexibility of the vehicle, it has disadvantages such as complex structure, high cost and low efficiency [17-19].

To improve the maneuverability in hilly, mountainous and other unstructured roads and complex and diverse environments and enhance passage capacity and steering performance on atypical roads, this study has designed a mechanical dual power flow differential steering mechanism to achieve a constant turning radius. It is a newly invented differential steering mechanism that combines fixed-axis gear and planetary gear transmission with differential gears, making the driving wheels realize pure rolling motion. The overall structure of the steering mechanism is simple and centralized, with high transmission efficiency, high-speed steering, and high-stability linear driving. It cannot only adopt various driving forms (including motors and engines) but is also suitable for wheeled or tracked all-terrain military and civilian vehicles and various special equipment with mobile platforms, such as tractors, tanks, and desert vehicles. This study investigated the steering performance of arch waist agricultural travelling chassis by exploring the characteristics of dual power flow differential steering mechanisms.

The remaining paper is organized as follows: Section 2 presents the design of differential steering

Forest Chemicals Review
www.forestchemicalsreview.com
ISSN: 1520-0191
May-June 2022 Page No. 1348 – 1367
Article History: Received: 24 February 2022, Revised: 05 April 2022, Accepted: 08 May 2022, Publication: 30 June 2022

mechanism while section 3 presents the arch waist agricultural travelling chassis analysis. Section 4 presents the test structure analysis whereas the paper is concluded in Section 5.

II. DESIGN OF DIFFERENTIAL MECHANISM

Figure 1 shows the designed dual power flow differential steering mechanism, which consists of two rows of planetary gears, a planetary carrier, a differential steering mechanism housing, and left and right output semi shafts. The common differential housing and the sun gear #1 mesh with the planetary gear in the first planetary row; the sun gear #2 connected to the right semi shaft meshes with the planetary gear in the second planetary row; the engage gear ring of the first planetary row is fixedly connected to the differential steering mechanism housing; the planetary carrier of the first planetary row is connected to the planetary carrier of the second planetary row, i.e., they share the same planetary carrier; the engage gear ring of the second planetary row is fixedly connected to the first gear.

1- left semi shaft; 2- right semi shaft; 3-driving bevel gear; 4- planetary gear shaft; 5- planetary gear #1; 6- common differential housing; 7- left semi shaft gear; 8- planetary gear #2; 9- differential steering mechanism housing; 10-driven bevel gear; 11- right semi shaft gear; 12-gear ring #1; 13- planetary gear #3; 14- gear ring #2; 15- planetary gear #4; 16- gear #1; 17- sun gear #1; 18- sun gear #2; 19- dual planet carrier; 20- gear #2; 21- steering drive motor

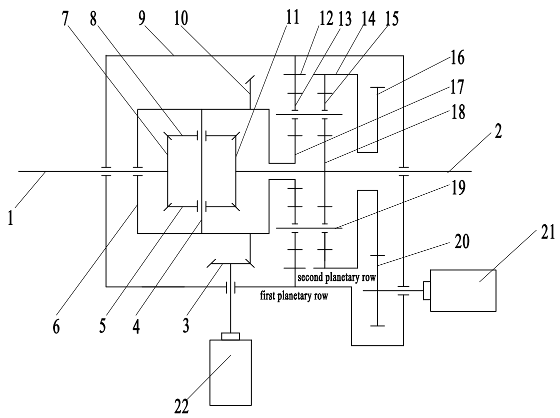

Fig 1: Schematic diagram of the structure of the differential steering mechanism.

In the process of differential steering, there are two power inputting into the steering mechanism, one from the engine output through the driving bevel gear and the other from the steering drive motor. These two powers merge in the differential steering mechanism. The power flow input by the engine makes the two semi shafts rotate at the same rotational velocity to move forward or backward. The power flow input by the steering motor can increase the rotational velocity of the output shaft on one side and reduce the rotational

Forest Chemicals Review
www.forestchemicalsreview.com
ISSN: 1520-0191
May-June 2022 Page No. 1348 – 1367
Article History: Received: 24 February 2022, Revised: 05 April 2022, Accepted: 08 May 2022, Publication: 30 June 2022

velocity of the output shaft on the other side simultaneously. The increased or decreased value of the two output shafts is the same so that the rotational velocity difference between the two output shafts can achieve the differential steering.

By adjusting the rotational velocity and direction of the input shafts that control the two power flows, the arch waist travelling chassis can be controlled to turn left and right with different radii. Generally speaking, there are three different operating conditions for the differential steering mechanism:

1) The gearbox works, but the steering drive motor does not work;

2) The gearbox does not work, and the steering drive motor works;

3) The gearbox and the steering drive motor work simultaneously.

The prototype of the differential steering mechanism is shown in Figure 2.

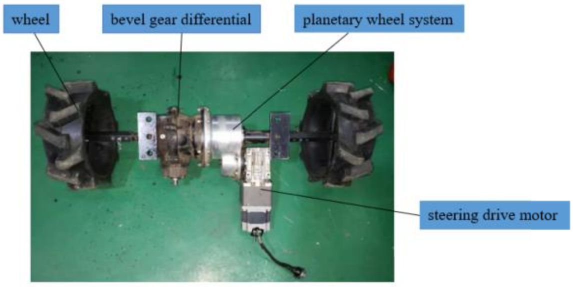

Fig 2: Prototype of the differential steering mechanism.

2.1 Chassis Structure of the Arch Waist Agricultural Travelling Chassis

The principle of the transmission system of the arch waist agricultural travelling chassis is shown in Figure 3. The engine is connected to the gearbox. Part of the power from the gearbox is input to the driving wheels of the front track through the steering gear, which drives the track to rotate; part of the power is connected to the dual power flow differential steering mechanism. In the differential steering mechanism, the power from the engine and the power from the steering motor converge, and then it is transmitted from the left and right semi shafts to the left and right drive wheels connected to them. The chassis of the arch waist agricultural travelling chassis is mainly composed of a single track and two wheels on both sides. The compact and small walking mechanism makes it possible to operate in hilly and mountainous areas. Specifically, the track increases the contact area be-tween ground and vehicle, and the track and the two wheels construct a stable triangular structure, which ensures driving stability. The track and the wheels are flexibly articulated in the longitudinal plane, making the relative motion angle become the longitudinal profiling angle. The size of the angle varies within a certain range to realize the longitudinal profiling of the chassis to the ground.The arch waist agricultural machinery travelling chassis prototype is shown in Figure 4

Forest Chemicals Review
www.forestchemicalsreview.com
ISSN: 1520-0191
May-June 2022 Page No. 1348 – 1367
Article History: Received: 24 February 2022, Revised: 05 April 2022, Accepted: 08 May 2022, Publication: 30 June 2022

TABLE I. Parameters used in this study.

Parameter	Numeric value
Length x width x height (mm x mm x mm)	1280x950x820
Pitch x number of pitches x width (mm x mm x mm)	60x60x150
Weight (kg)	300
Center distance between the driving wheel and rear wheel (mm)	600
Wheelbase (mm)	850
Track driving wheel radius (mm)	160
Rear wheel radius (mm)	170
Rear wheel width (mm)	100

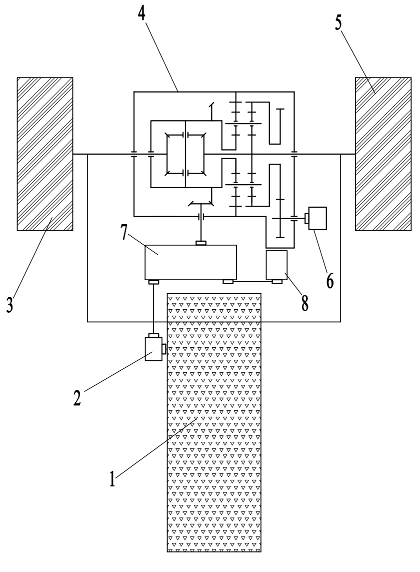

1- Track; 2- Steering gear; 3- Left drive wheel; 4- Differential steering mechanism; 5- Right drive wheel; 6- Steering drive motor; 7- Gearbox; 8- Engine.

Fig 3: Schematic diagram of the transmission route of the arch waist travelling chassis.

Forest Chemicals Review
www.forestchemicalsreview.com
ISSN: 1520-0191
May-June 2022 Page No. 1348 – 1367
Article History: Received: 24 February 2022, Revised: 05 April 2022, Accepted: 08 May 2022, Publication: 30 June 2022

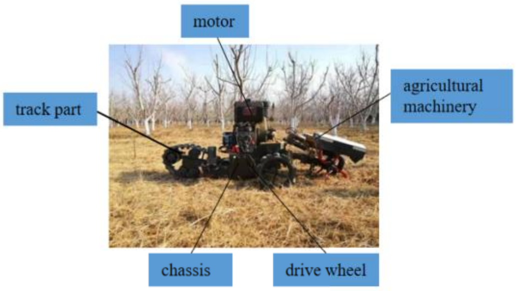

Fig 4: Prototype of arch waist travelling chassis.

2.2 Analysis of Steering Performance

Based on the characteristics of planetary gears and Figure 1, the rotational velocities of the components of the differential steering mechanism can be obtained:

$$n_1 + n_2 = n_6 \tag{1}$$

$$n_{17} + \alpha n_{12} - (1+\alpha) n_{19} = 0 \tag{2}$$

$$n_{18} + \alpha n_{14} - (1+\alpha) n_{19} = 0 \tag{3}$$

where, n_1 denotes the rotational velocity of the left semi shaft; n_2 denotes the rotational velocity of the right semi shaft; n_6 denotes the rotational velocity of the driven gear of the main reducer; n_{17} denotes the rotational velocity of the sun gear #1; n_{18} denotes the rotational velocity of the sun gear #2; n_{12} denotes the rotational velocity of the gear ring #1; n_{14} denotes the rotational velocity of the gear ring #2; n_{19} denotes the rotational velocity of the planetary carrier. α is the characteristic parameter of the planetary row (the ratio of the number of the gear ring teeth to the number of sun gear teeth).

Based on (1) ~ (3), the rotational velocity of the wheels on the left and right sides of the arch waist agricultural travelling chassis can be obtained:

$$\begin{cases} n_1 = \dfrac{i_b i_d n_{f1} + \alpha i_a i_c n_{f2}}{i_a i_b i_c i_d} \\ n_2 = \dfrac{i_b i_d n_{f1} - \alpha i_a i_c n_{f2}}{i_a i_b i_c i_d} \end{cases} \tag{4}$$

where, i_a denotes the transmission ratio of the driving gear to the driven gear of the main reducer; i_b denotes the transmission ratio of the driving gear to the large spur gear of the steering drive motor; i_c denotes the transmission ratio of the gearbox, i_d denotes the steering drive motor output shaft to reducer transmission ratio; n_{f1} denotes the output rotational velocity of the engine; n_{f2} denotes the output

Forest Chemicals Review
www.forestchemicalsreview.com
ISSN: 1520-0191
May-June 2022 Page No. 1348 – 1367
Article History: Received: 24 February 2022, Revised: 05 April 2022, Accepted: 08 May 2022, Publication: 30 June 2022

rotational velocity of the steering drive motor.

The relationship between the rotational velocity of the left and right driving wheels of the tracked vehicle and the rotational velocity of the left and right output semi shafts of the differential steering mechanism is as follows:

$$\omega_k = \frac{\pi n_i}{30}, i = 1, 2 \quad (5)$$

In a certain gear, when the characteristic parameters of the planetary row of the steering mechanism are the same, the relationship between the rotational velocity of the left and right driving wheels and the rotational velocity of the steering motor is shown in Figure 5. O_1 denotes the instantaneous speed of the Arch Waist agricultural travelling chassis. When O_1 moves to O (the output rotational velocity of the gearbox is zero), the left and right drive wheels rotate at equal rotational velocity and in opposite directions, and the arch waist agricultural travelling chassis performs the in-situ steering.

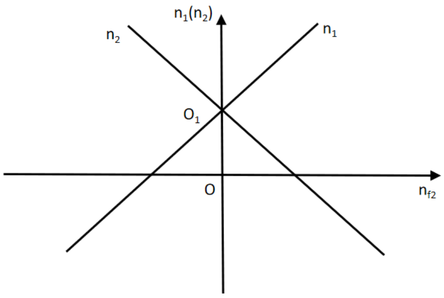

Fig 5: The rotational velocity of the driving wheel and the steering drive motor in a certain gear.

The rotational velocity of the engine and the steering drive motor and directions of the rotational velocities of left and right wheels under various working conditions of the dual power flow steering mechanism of the Arch Waist agricultural travelling chassis is shown in Table I. Here, "+" denotes clockwise direction, "-" denotes counterclockwise direction, "0" means that the rotational velocity is zero.

TABLE Ⅱ. Working conditions of the gearbox and driving motor of the arch waist agricultural travelling chassis.

Working conditions	Rotational velocity of gearbox	Rotational velocity of drive motor
Linear driving	+	0
Counterclockwise turn (forward)	+	+
Clockwise turn (forward)	+	-
Counterclockwise turn (backward)	-	+
Clockwise turn (backward)	-	-
Counterclockwise turn (in-situ)	0	+

Forest Chemicals Review
www.forestchemicalsreview.com
ISSN: 1520-0191
May-June 2022 Page No. 1348 – 1367
Article History: Received: 24 February 2022, Revised: 05 April 2022, Accepted: 08 May 2022, Publication: 30 June 2022

Clockwise turn (in-situ)	0	-

It can be seen from Formula (4) and Table Ⅱ that the rotational velocities of the left and right driving wheels can be controlled by manipulating the rotational velocities and the directions of the steering motor to improve the three driving states of the Arch Waist travelling chassis.

Supposing the rotational velocities of the left and right drive wheels are known, the transmitting ratio of the gearbox and the rotational velocity of the steering drive motor can be obtained based on Formula (5) to make the Arch Waist travelling chassis steer at a certain speed.

$$\begin{cases} n_{f1} = \dfrac{i_c(n_1 + n_2)}{2 i_a} \\ n_{f2} = \dfrac{i_b i_d (n_1 - n_2)}{2\alpha} \end{cases} \tag{6}$$

As can be seen from Formula (6), the output rotational velocity of the gearbox determines the average value of the sum of the rotational speeds of the left and right drive wheels, and has nothing to do with the driving state and steering direction of the Arch Waist agricultural travelling chassis. The rotational speed of the steering drive motor is proportional to the difference between the rotational velocities of the left and right drive wheels and is independent of its specific values.

III. ARCH WAIST AGRICULTURAL TRAVELLING CHASSIS ANALYSIS

3.1. Steering Kinematic Analysis of Arch Waist Agricultural Travelling Chassis

To facilitate the establishment of a reasonable kinematic model of the arch waist agricultural travelling chassis, the model has been reasonably simplified:

1) We assume that the components of the arch waist agricultural travelling chassis are rigid bodies and will not deform;

2) The steering speed of the arch waist agricultural travelling chassis is slow, with low centrifugal force, which can be ignored;

3) The arch waist agricultural travelling chassis center of mass coincident with its geometric center.

When the arch waist agricultural travelling chassis turns, its front track lifts, which can be regarded as the contact between the driving wheel and the ground.

The special structure of the arch waist agricultural travelling chassis with tracks in front and wheels in the back makes the kinematic model containing numerous soil parameters very complex, which generates frequent skid and slip between the ground and the vehicle. This study adopted the method based on the instantaneous center of rotation to establish the kinematic model of the arch waist agricultural travelling

Forest Chemicals Review
www.forestchemicalsreview.com
ISSN: 1520-0191
May-June 2022 Page No. 1348 – 1367
Article History: Received: 24 February 2022, Revised: 05 April 2022, Accepted: 08 May 2022, Publication: 30 June 2022

chassis.

We established a coordinate system as shown in Figure 6, where XOY denotes the geodetic coordinate system, O denotes the steering center of the arch waist agricultural travelling chassis, O_1 denotes the geometric center of the arch waist agricultural travelling chassis, R_0 denotes the turning radius, ω denotes the steering angular velocity, and rm denotes the radius of the driving wheel.

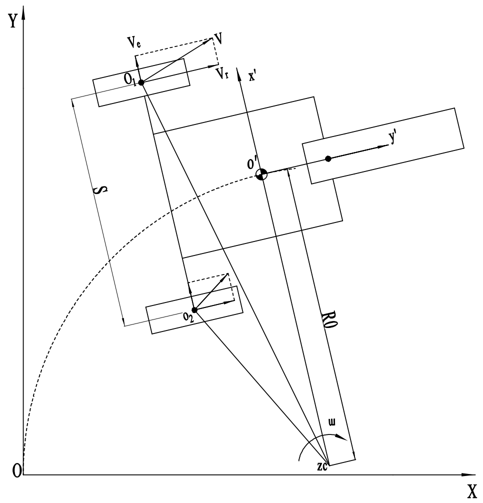

Fig 6: Schematic diagram of the turning of the arch waist agricultural travelling chassis when walking.

$$\frac{v_L}{v_R} = \frac{R_0 - 0.5s}{R_0 + 0.5s} \tag{7}$$

Where, S denotes the distance between the two rear wheels, V_L, V_R denotes the rotational speeds of the left and right driving wheels, respectively. When the arch waist agricultural travelling chassis steers steadily at low speed on the horizontal ground, the longitudinal offset of the steering pole of the entire vehicle is small and usually can be neglected, and the turning radius can be obtained from Formulae (4) and (7).

$$R_0 = -\frac{S i_b i_d n_{f1}}{2\alpha i_a i_c n_{f2}} \tag{8}$$

To verify that the differential steering mechanism can achieve accurate steering, the turning radius of the arch waist agricultural travelling chassis was studied using the engine output shaft of the differential steering mechanism and the motor shaft of the steering drive as the power input.

Forest Chemicals Review
www.forestchemicalsreview.com
ISSN: 1520-0191
May-June 2022 Page No. 1348 – 1367
Article History: Received: 24 February 2022, Revised: 05 April 2022, Accepted: 08 May 2022, Publication: 30 June 2022

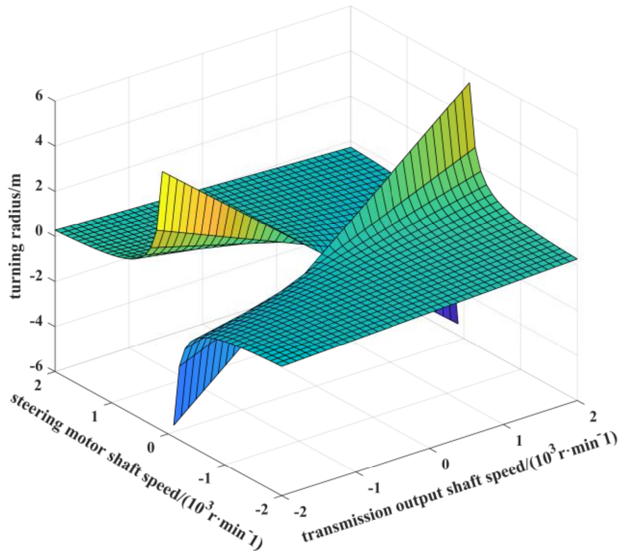

Fig 7: The relationship between the turning radius (R_0) and the output shaft of the gearbox (n_{f1}) and the shaft of the steering drive motor (n_{f2}).

According to Formula (8), the turning radius (R_0) is affected by the output rotational velocity of the engine and the rotational velocity of the steering drive motor. As shown in Figure 7, the turning radius increases with the increase of the output shaft rotational velocity of the engine and decreases with the increase of the output shaft rotational velocity of the steering drive motor. As shown in Figure 8, the rotational velocities of the steering drive motor shaft are set to $\pm 500 r/min, \pm 1000 r/min, \pm 1500 r/min$. Clockwise is defined as positive, and counterclockwise is defined as negative. When the rotational speed of the steering drive motor shaft $n_{f2} > 0 r/min$, the change of the gearbox output shaft rotational speed and the turning radius of the arch waist agricultural travelling chassis is shown in Figure 8(a). When the gearbox output shaft rotational velocity $n_{f1} > 0 r/min$ (or $n_{f1} < 0 r/min$), the turning radius of the arch waist agricultural travelling chassis increases as the rotational velocity of the gearbox output shaft increases, and the arch waist agricultural travelling chassis turns counterclockwise; when the rotational velocity of the steering drive motor shaft $n_{f1} > 0 r/min$, the rotational velocity of the gearbox output shaft and turning radius of arch waist agricultural travelling chassis is shown in Figure 8(b). When the rotational velocity of the gearbox output shaft $n_{f1} > 0 r/min$ (or $n_{f1} < 0 r/min$), the turning radius of the arch waist agricultural travelling chassis increases with the increase of the gearbox output shaft rotational velocity, and the arch waist agricultural travelling chassis turns clockwise; when the rotational velocity of the gearbox output shaft $n_{f1} = 0 r/min$ and the turning radius $R_0 = 0m$, the left and right driving wheels rotate at the same velocity in opposite directions, and the arch waist agricultural travelling chassis turns counterclockwise (clockwise) and performs in-situ steering.

Forest Chemicals Review
www.forestchemicalsreview.com
ISSN: 1520-0191
May-June 2022 Page No. 1348 – 1367
Article History: Received: 24 February 2022, Revised: 05 April 2022, Accepted: 08 May 2022, Publication: 30 June 2022

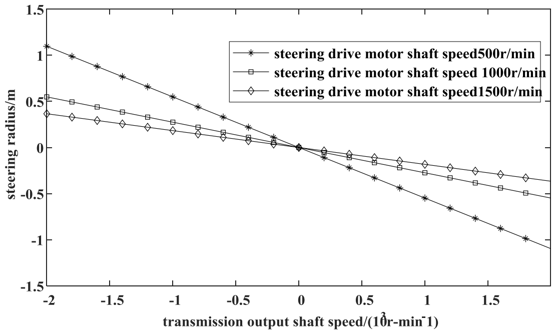

Fig 8 (a): Steering drive motor shaft rotational velocity $n_{f2} > 0$.

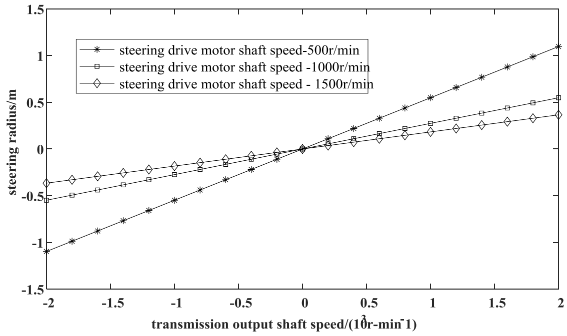

Fig 8 (b): Steering drive motor shaft rotational velocity $n_{f2} < 0$.

The influence of the rotational velocity of the steering drive motor shaft on the turning radius is shown in Figure 9. To analyze the influence of the rotational velocity of the steering drive motor shaft on the turning radius, the output shaft rotational velocity of the gearbox is set to $\pm 500r/min, \pm 1000r/min, \pm 1500r/min$. Clockwise is de-fined as positive, and counterclockwise is defined as negative. When the rotational velocity of the gearbox output shaft $n_{f1} > 0r/min$, the change of the steering drive motor shaft rotational velocity and the turning radius of the arch waist agricultural travelling chassis are shown in Figure 9 (a). When the rotational velocity of the steering drive motor shaft is $n_{f2} > 0r/min$ (or $n_{f2} < 0r/min$), the turning radius of the arch waist agricultural travelling chassis decreases as the rotational velocity of the steering drive motor shaft increases, and the arch waist agricultural travelling chassis turns counterclockwise (clockwise). When the rotational velocity of the gearbox output shaft is $n_{f1} < 0r/min$, the change of the steering drive motor shaft rotational velocity and the turning radius of the arch waist agricultural travelling chassis is shown in Figure 9(b). When the rotational velocity of the steering drive motor shaft is $n_{f2} > 0r/min$ (or $n_{f2} < 0r/min$), the turning radius of the arch waist agricultural travelling chassis decreases with the increase of the rotational velocity of the steering drive motor shaft, and the arch waist agricultural travelling chassis turns counterclockwise (clockwise). When the rotational velocity of the steering drive motor shaft is $n_{f2} = 0r/min$ and the turning radius is $R_0 \to \infty$, the rotational velocities of the left and right drive wheels are equal with the same direction, and the arch waist agricultural travelling chassis moves forward or backward.

Forest Chemicals Review
www.forestchemicalsreview.com
ISSN: 1520-0191
May-June 2022 Page No. 1348 – 1367
Article History: Received: 24 February 2022, Revised: 05 April 2022, Accepted: 08 May 2022, Publication: 30 June 2022

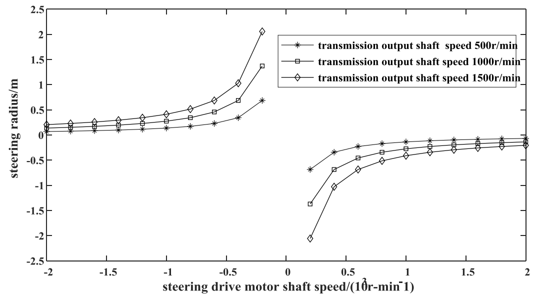

Fig 9(a): Gearbox output shaft rotational velocity $n_{f1} > 0$

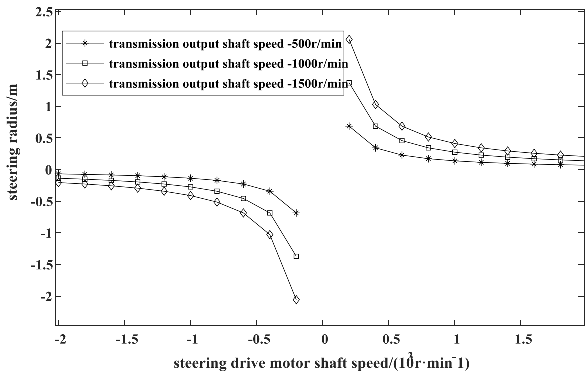

Fig 9(b): Gearbox output shaft rotational velocity $n_{f1} < 0$

In conclusion, when the rotational velocity of the steering motor shaft is constant, the turning radius of the arch waist agricultural travelling chassis increases with the increase of the rotational velocity of the gearbox output shaft; when the rotational velocity of the gearbox output shaft is constant, the turning radius of the arch waist agricultural travelling chassis decreases with the increase of the rotational velocity of the steering drive motor shaft, and the arch waist agricultural travelling chassis can perform any constant turning radius (including in-situ turning).

3.2. Dynamic Analysis of the Steering Mechanism of the Arch Waist Agricultural Travelling Chassis

In the dynamics model of the differential steering mechanism, the driving torques acting on the left and right wheels are

$$\begin{cases} M_{17} = \dfrac{M_{12}}{\alpha} = \dfrac{M_{13}}{-(1+\alpha)} \\ M_{18} = \dfrac{M_{14}}{\alpha} = \dfrac{M_{15}}{-(1+\alpha)} \end{cases} \tag{9}$$

Where α denotes the characteristic coefficient of the planetary row; M_{17}, M_{12}, M_{13} are the torque exerted

Forest Chemicals Review
www.forestchemicalsreview.com
ISSN: 1520-0191
May-June 2022 Page No. 1348 – 1367
Article History: Received: 24 February 2022, Revised: 05 April 2022, Accepted: 08 May 2022, Publication: 30 June 2022

by the planetary gears in the first planetary row on the sun gear, gear ring and planetary carrier; M_{18}, M_{14}, M_{15} are the torque exerted by the planetary gears in the second planetary row on the sun gear, gear ring and planetary carrier. Based on the moment balance condition and Formula (9), we can obtain:

$$\begin{cases} M_1 = \dfrac{M_3}{2i_a} - \dfrac{M_{20}}{2\alpha i_b} \\ M_2 = \dfrac{M_3}{2i_a} + \dfrac{M_{20}}{2\alpha i_b} \end{cases} \tag{10}$$

Based on the torques of the left and right output shafts M1 and M2 and Formula (10), we can obtain:

$$\begin{cases} M_3 = i_a(M_1 + M_2) \\ M_{20} = \alpha i_b(M_2 - M_1) \end{cases} \tag{11}$$

According to Formula (11), the output semi-shaft torque at both ends of the differential steering mechanism is related to the output torque of the gearbox and the output torque of the steering drive motor, but has nothing to do with other components of the steering drive mechanism. When the arch waist agricultural travelling chassis moves in a straight line, the input torque of the steering drive motor $M_{20} = 0$, the engine works alone, and the output torque of the left and right semi shafts is equal in size and direction. When the driving conditions on the left and right sides of the road are the same, the torque input from the gearbox is equally distributed to the two output semi shafts to complete the final transmission, so that the differential steering mechanism has the function of equal torque distribution. Under linear driving $n_1 = n_2$,the steering drive motor does not provide power. When the vehicle is unbalanced $M_1 \neq M_2$, the steering drive motor bear's torque. As shown in Figures 10(a) (b), when the arch waist agricultural travelling chassis performs in-situ steering, the engine input torque $M_3 = 0$, the steering drive motor works, the input torque of the left and right semi shafts is the same with the opposite directions, the turning radius is 0. In this case, the arch waist agricultural travelling chassis rotates in situ with the contact area between the track driving wheel and the ground as the center of the circle. When the engine and the steering drive motor input torque simultaneously, the arch waist agricultural travelling chassis will drive while steering. When the arch waist agricultural travelling chassis moves in a straight line, the input torque of the steering drive motor $M_{20} = 0$, the engine works alone, and the output torque of the left and right semi shafts is equal in size and direction. That is, the arch waist agricultural travelling chassis does not change the driving direction, and continues to move along the original direction. When the engine and the steering drive motor input torque simultaneously, the arch waist agricultural travelling chassis drives while steering. The arch waist agricultural travelling chassis can move forward and backward at different speeds by shifting the gearbox between high and low gears and reverse gear. The magnitude and direction of the input torque of the steering drive motor make the torque of one output semi shaft increase and another decrease with the same value. By adjusting the rotational velocity and the direction of the steering drive motor, the arch waist agricultural travelling chassis can move to the left or right with different radii and drive while turning (including in-situ steering).

Forest Chemicals Review
www.forestchemicalsreview.com
ISSN: 1520-0191
May-June 2022 Page No. 1348 – 1367
Article History: Received: 24 February 2022, Revised: 05 April 2022, Accepted: 08 May 2022, Publication: 30 June 2022

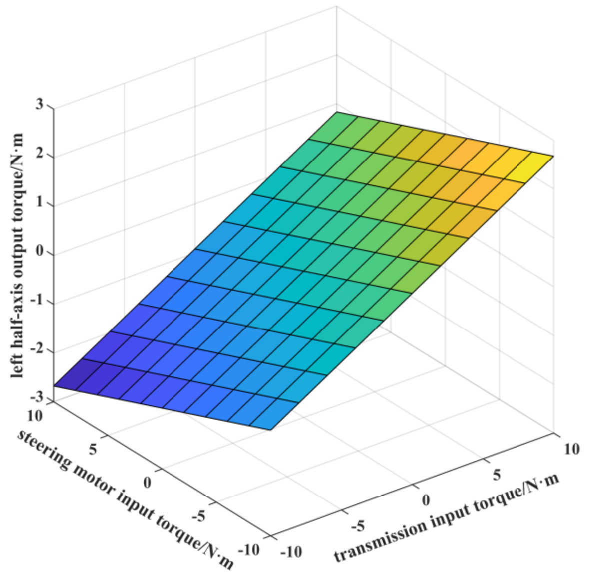

Fig 10 (a): The relationship between the input torque of the gearbox and steering motor and the output torque of the left semi shaft.

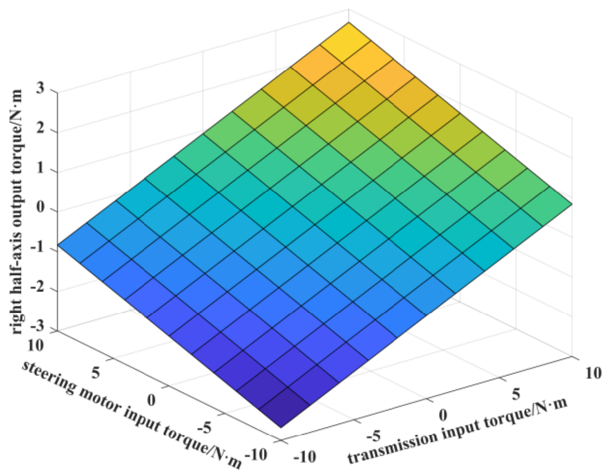

Fig 10 (b): The relationship between the input torque of the gearbox and steering motor and the output torque of the right semi shaft.

3.3. Theoretical Maximum Steering Angular Velocity

The steering angular velocity of the arch waist agricultural travelling chassis is maximum when the rotational velocity of the gearbox is zero, the two drive wheels on the rear side rotate in opposite directions, and the steering angular velocity of the steering mo-tor is the highest. According to Figure 11, we can obtain:

$$\omega_{max}(rad \cdot s^{-1}) = \frac{v_1}{L} = \frac{2\pi r n_1}{60L} \tag{12}$$

Forest Chemicals Review
www.forestchemicalsreview.com
ISSN: 1520-0191
May-June 2022 Page No. 1348 – 1367
Article History: Received: 24 February 2022, Revised: 05 April 2022, Accepted: 08 May 2022, Publication: 30 June 2022

When $n_{f1} = 0$, $n_1 = \dfrac{\alpha n_{f2}}{i_b i_d}$

By substituting it into Formula (12), we can obtain

$$\omega_{max}(rad \cdot s^{-1}) = \frac{\pi r \alpha n_{f2}}{30 i_b i_d L} \tag{13}$$

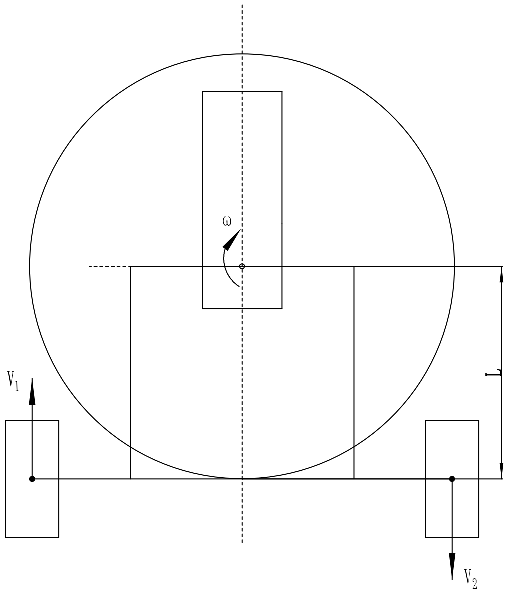

Fig 11: Theoretical minimum turnaround angular velocity

It can be concluded from Formula (12) that when the gearbox does not input power, the steering angular velocity is proportional to the input velocity of the steering motor; that is, the steering angular velocity increases with the increase of the input velocity of the steering motor. However, the steering angular velocity is affected by the ground adhesion, which makes the vehicle easy to skid, thus increasing the turning radius and reducing the steering angular velocity.

3.4. Theoretical Minimum Turnaround Time

The turnaround time refers to the time required for the arch waist agricultural travelling chassis to revolve around the contact area between its front track and the ground. The minimum turnaround time is:

$$t_{min} = \frac{2\pi}{\omega_{max}} = \frac{60 i_b i_d L}{\alpha r n_{f2}} \tag{14}$$

Ⅳ. ARCH WAIST AGRICULTURAL TRAVELLING CHASSIS ANALYSIS

To verify the correctness of the theoretical results, the dual power flow differential steering

Forest Chemicals Review
www.forestchemicalsreview.com
ISSN: 1520-0191
May-June 2022 Page No. 1348 – 1367
Article History: Received: 24 February 2022, Revised: 05 April 2022, Accepted: 08 May 2022, Publication: 30 June 2022

mechanism of the arch waist agricultural travelling chassis was tested on the concrete pavement and farmland [20-22], and the theoretical minimum turning radius and the theoretical minimum turnaround time were experimentally trialed [23-25].

4.1 Straight-Line Performance Test

As per the military tracked straight-line driving performance method, the straight-line performance of the prototype was tested, with concrete pavement as the road conditions and tape measure, chalk, range pole as the instrument and equipment. We parked the prototype on the selected road, marked a straight line forward with the edge of the tire on one side as the baseline. The front end of the first track plate was taken as the starting point when the contact area between the ground and the front track drive mechanism was maximum. Then, we made a mark at 50 meters away from the starting point along the baseline and drew a horizontal plumb line at the position of the mark. Then we made the prototype move at a constant speed in low gear. Only the engine that controlled the straight line worked, and the motor that controlled the steering did not work. When the prototype reached the endpoint, we measured the vertical distance deviating from the baseline, recorded the deviation distance. We repeated the above actions three times and got the yaw rate by taking the average value.

$$p = \frac{e}{l} \times 100\% \qquad (15)$$

where e denotes the deviation distance (m), l denotes the calibration distance (m).

The leftward deviation is defined as positive, and the deviation distance is 0.41 m, 0.43 m, -0.39 m, respectively. According to Formula 14, the average yaw rate is 0.82%. The GJB 4111.5-2000 specifies that the yaw rate shall not exceed 1%. The test indicated that the yaw rate of the prototype is within the range of the national standard; that is, the mechanical dual power flow differential steering mechanism has good linear walking performance when not steering.

4.2 Minimum turning radius test

Test method: The 5905-test system was used to test the rotational velocity of the left and right output semi shafts. Four strain gauges (model BFH120) were attached to the left and right output semi shafts. The strain gauges were arranged in a double horizontal splayed layout with a full bridge connection circuit. After calibration, they were connected with the acquisition module of the 5905-test system, and then the data were transferred to the computer acquisition software via a wireless router Tp-link to realize real-time monitoring of the prototype's rotational velocity [26-28].

For field cultivation in hilly and mountainous areas, steering performance is more important than straight-line stability. By controlling the track of the arch waist agricultural robot, the track is lifted during the steering process to reduce contact with the ground, thus lowering the frictional resistance. When the engine shaft and the steering drive motor shaft work simultaneously, the output rotational velocity of the left and right half shafts is the superposition of the two input rotational velocities, and the arch waist

Forest Chemicals Review
www.forestchemicalsreview.com
ISSN: 1520-0191
May-June 2022 Page No. 1348 – 1367
Article History: Received: 24 February 2022, Revised: 05 April 2022, Accepted: 08 May 2022, Publication: 30 June 2022

agricultural robot steers while driving. When the engine shaft shifts to neutral gear, the steering drive motor inputs the rotational speed. At this point, the left and right semi shafts rotate in the opposite direction to perform the in-situ steering with the contact point between the track and the ground as the pivot.

The test was conducted on the concrete pavement and the farmland, and the rotational velocity of the driving wheel was 11 r/min, 22 r/min and 34 r/min, respectively. Figure 12 shows the in-situ steering test on the concrete pavement, and Figure 13 shows the test on the farmland.

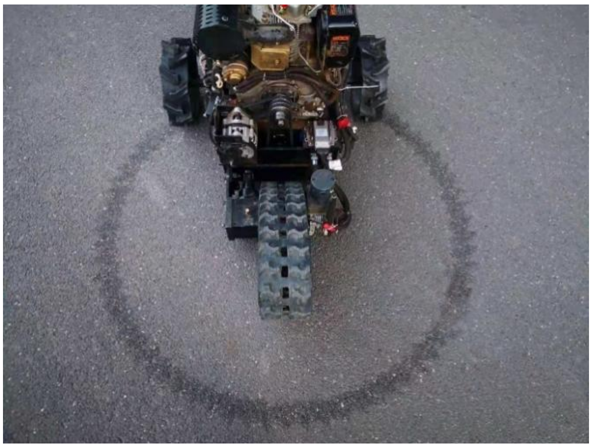

Fig 12: Test diagram of in-situ steering on concrete pavement.

Fig 13: Diagram of test on farmland.

Table Ⅲ shows the measurement results of the minimum turning radius of the prototype on the concrete pavement, and Table Ⅳ shows the measurement results of the minimum turning radius of the prototype on the farmland.

TABLE Ⅲ. Measurement results of the minimum turning radius on the concrete pavement.

No.	Steering angular speed ω/(rad · s

Forest Chemicals Review
www.forestchemicalsreview.com
ISSN: 1520-0191
May-June 2022 Page No. 1348 – 1367
Article History: Received: 24 February 2022, Revised: 05 April 2022, Accepted: 08 May 2022, Publication: 30 June 2022

	-1)		
	0.33	0.67	1
1	0.032	0.030	0.038
2	0.031	0.035	0.032
3	0.033	0.037	0.028
Mean		0.033	

TABLE Ⅳ. Measurement results of the minimum turning radius on the farmland.

No.	**Steering angular velocity ω/(rad · s -1)**		
	0.33	0.67	1
1	0.036	0.039	0.051
2	0.033	0.037	0.045
3	0.034	0.040	0.049
Mean		0.040	

It can be seen from Tables Ⅲ and Table Ⅳ that during the mechanical dual power flow differential steering, the wheels on both sides rotate at the same velocity. Due to the different skid and slip of the wheels on both sides, the turning radius is not zero, but it is much smaller than that of traditional steering. The minimum turning radius of the prototype on the concrete pavement is 0.033 m, and the minimum turning radius of the prototype on the paddy field is 0.040 m.

Ⅴ. CONCLUSION

The conclusion of the proposed model is derived in five parts:

1) With the newly invented agricultural travelling chassis as the power chassis, we designed a mechanical dual power flow differential steering mechanism. We established the dynamics model of the differential steering mechanism during the driving and steering of the arch waist agricultural travelling chassis based on an analysis of the working mechanism of the dual power flow differential steering mechanism. We also derived the theoretical model of the input rotational velocity of the gearbox output shaft and the steering motor shaft of the differential steering mechanism, and the output rotational velocity of the two semi shafts, providing the theoretical basis for the structural design and parameter selection and control of the differential steering mechanism.

2) The dual power flow differential steering mechanism facilitated the movement of the arch waist agricultural travelling chassis by enabling it to steer at any radius, significantly improving its driving mobility. Additionally, with no reduction in driving speed during steering, the arch waist agricultural travelling chassis can work as efficiently as it moves in a straight line.

3) We established the dynamics model of the dual power flow differential steering mechanism of the arch waist agricultural travelling chassis, derived the torque equation, and pro-vided the theoretical basis for the selection of steering drive motor parameters and force analysis.

4) The prototype was tested for straight-line driving on the road. When the mechanical dual power flow differential steering mechanism did not perform steering, i.e., when the steering control was not used to correct the deviation, the yaw rate of straight-line performance was 0.82%, which met the national standard.

5) The results of the steering performance tests on the prototype revealed that the mechanical dual power flow differential steering mechanism has good performance. The drive wheel rotational velocities were set as 11 r/min, 22 r/min, and 34 r/min for the minimum radius tests on concrete pavements and farmland. The average mini-mum turning radius of the prototype on the concrete pavement was 0.033 m, making the vehicle have good maneuvering flexibility when turning. The average minimum turning radius of the prototype on the farmland was 0.040 m, significantly reducing the contact area between the ground and the vehicle when turning.

ACKNOWLEDGEMENTS

This research was supported by the National Natural Science Foundation of China Youth Science Foundation Project (Grant No.51905154).

REFERENCES

[1] Wang, S.S; Geng, L.X. (2016) Development Situation and Countermeasures of Agricultural Mechanization in Hilly and Mountain Areas. Agricultural Engineering 6(5):1-4.
[2] Jiang, X.L; Chi, Z.Z, Li, X.Y. (2012) Question and Solution for Development of Agriculture Mechanization in Hilly and Mountainous Region. Chinese Agricultural Mechanization (6):12-14.
[3] Ma, X.; Li, Y.M.; Tang, Z.; Huang, J.; Zhu, L.H.(2018)Structural Features and Developing Tendency of the Steering Mechanism for the Crawler Combine Harvester. Journal of Agricultural Mechanization Research 40(4):1-6, 25.
[4] Chi, Y.; Zhang, H.Q.; Quan, L.Z.; Jiang, E.C. (2012) Theoretical Study on Differential Steering Performance of Agricultural Tracked Vehicle. Journal of Northeast Agricultural University. 43(5):50-54.
[5] Al-Milli, S.; Seneviratne, L.D.; Althoefer, K. (2010) Track–terrain modeling and traversability prediction for tracked vehicles on soft terrain. Journal of Terramechanics. 47(3):151-160.
[6] Ullah, I.; Yu, S.; Xin, S.; Esposito, C.; Chang C. "A localization based on unscented Kalman filter and particle filter localization algorithms." IEEE Access 8 (2019): 2233-2246.
[7] Chen, Z.F.; Xie, X.L.; Gao, F.; Liu, Z.Y.; Li, Y.Y. "Pure Rolling Steering System Design and Research for Wheeled Mobile Ro-bot." In Journal of Physics: Conference Series, vol. 1345, no. 4, p. 042071. IOP Publishing, 2019.
[8] Inam, U.; Qian, S.Y; Deng, Z.X.; Lee, J.H. (2021)"Extended Kalman Filter-based localization algorithm by edge computing in Wire-less Sensor Networks." Digital Communications and Networks 7(2)187-195.
[9] Solis, J.M.; Longoria, R.G. (2008) Modeling track–terrain interaction for transient travelling chassisic vehicle maneuvers. Journal of Terramechanics. 45(3):65-78.
[10] Liu, Y.G.; Liu, G.J. (2009) Modeling of tracked mobile manipulators with consideration of track-terrain and vehicle-manipulator interactions. Travelling chassisics and Autonomous Systems. 57(11):1065-74.

Forest Chemicals Review
www.forestchemicalsreview.com
ISSN: 1520-0191
May-June 2022 Page No. 1348 – 1367
Article History: Received: 24 February 2022, Revised: 05 April 2022, Accepted: 08 May 2022, Publication: 30 June 2022

[11] Wong, J.Y.; Huang, W. (2008) Approaches to improving the mobility of military tracked vehicles on soft terrain. Heavy vehicle systems. 15(2/4):127-51.
[12] Wong, J.Y.; Jiang, C.F. (2001) A general theory for skid steering of tracked vehicles on firm ground. Proceedings of the Institution of Mechanical Engineers, Part D. Journal of Automobile Engineering. 215(3):343-55.
[13] Xiong, G.M.; Lu, H.; Guo, K.H.; Chen, H.Y. (2017) Research on Trajectory Prediction of Tracked Vehicles Based on Real Time Slip Estimation. Acta Armamentarii. 38(3):8.
[14] Dong, C.; Cheng, K.; Gao, X.L.; Xi, Y.; Deng, Z.Y. (2017) Performance analysis of sliding steering of tracked vehicles under the in-fluence of centrifugal force. Journal of Vibration, Measurement & Diagnosis. 37(1):8.
[15] Feng, J.; Jiang, Y.Y. (2013) Mechanism and performance test of unilateral drive in-situ steering mechanism of rice combine harvester. Transactions of the Chinese Society of Agricultural Engineering. 29(4):6.
[16] Yang H.Z. Analysis of virtual prototype of differential steering mechanism of tracked vehicles based on ADAMS. Master's thesis,Shandong University of Technology,Shandong,2010.
[17] Shi, Z.B.; Liu, J.; Gao, F.; Zeng, W. (2019) Steering performance of tracked vehicle based on mechanical differential steering mechanism with twin driving. Journal of Central South University (Science and Technology). 50(4):864-872.
[18] Cao F.Y.; Zhou, Z.L. (2006) Design of Hydromechanical Double Power Differential Steering Mechanism for Tracked Tractor. Trans-actions of the Chinese Society for Agricultural Machinery. 37(9):5-8.
[19] Cao, F.Y.; Zhou, Z.L.; Zhao, H.J. (2012) Design of Steering Wheel Control System of Tracked Vehicle of Hydro-Mechanical Differential Turning Advanced Materials Research. 472-475:753-756.
[20] Rui, Q.; Wang H.Y.; Wang, Q.L.; Wan, L.; Gai J.T.; Zhou, G.M. (2015) Research on the Acquisition of Steering Performance Parameters of Armored Vehicle Based on Experiments. Journal of Mechanical Engineering. 51(12):127-136.
[21] Cheng, J.W.; Gao, L.H., Wang, H.Y. (2006) Steering analysis of tracked vehicles based on skid condition. Chinese Journal of Mechanical Engineering. 42(supp):192-195.
[22] Chi, Y. (2008) Performance Tests on Differential Steering Mechanism of Tracked Vehicle. Transactions of the Chinese Society for Agricultural Machinery. 39(7):14-17.
[23] Rubinstein, D., &Hitron, R. (2004) A detailed multibody model for dynamic simulation of offroad tracked vehicles.Journal of Terramechanics. 41(2/3):163-73.
[24] Ferretti, G.; Girelli, R. (1999) Modeling and simulation of an agricultural tracked vehicle. Journal of terramechanics 36(3):139-58.
[25] Zhang, J.; Jin, Q.; Wang, Q.; Zhang, P. (2018) Analysis and Simulation of Interaction Mechanism between Agricultural Tracked Vehicle and Ground. 2017 International Conference on Computer Systems, Electronics and Control (ICCSEC).IEEE.
[26] Li, Y.M.; Ye, X.F.; Xu, L.Z.; Pang, J.; Ma, Z. (2013) Construction and performance test of walking semi-axle load test system of com-bine harvester. Transactions of the Chinese Society of Agricultural Engineering. 29(006):35-41.
[27] Fang, Z.Q.; Gao, L.H.; Wang, H.Y. (2005) Indexes Analysis and Experimental Research on the Steering Performance of Tracked Vehicles. Journal of Academy of Armored Force Engineering. 19(4):5.
[28] Li, Y.M.; Chen, J.S.; Liang, Z.W.; Ma, X.; Jiang, X.C. (2016) Design and Experiment of Differential Steering Mechanism for Track Combine Harvester. Transactions of the Chinese Society for Agricultural Machinery. 47(7):8.